

The Quantitative Inversion of Iron Ore under Strong Constrain in Panzhihua-Baima Districts in Sichuan Province Based on the High-Precision Aeromagnetic Survey

Tengfei Ge^{1,2*}, Jingzi He^{1,2}, Xue Yang² and Xuzhao Huang²

¹ China University of Geosciences(Beijing);

² China Aero Geophysical Survey&Remote Sensing Center of land and resources.

Email:564465031@qq.com

Keywords: Magmatic iron ore, inversion, Panzhihua layered intrusion, South-West China

Abstract: The Panxi region in Sichuan province, Southwest China is famous for magmatic Fe-Ti-V oxide deposits in the country. The metallogenesis of the Panzhihua type V-Ti magnetite deposits remains controversial. Here we apply an interactive inversion technique on profiles of magnetic anomalies to study the deep geological structure of the Baima area. Combined with previous petrological and sedimentological studies on these rocks, the inversion results indicate that Baima iron deposits consist of several layered iron ore bodies. Different characteristics in the geometric forms of Panzhihua rock body and Baima rock body show different mineralization characters when forming magnetite ore layers under the gravity variation, resulting in different ore structures. Although the large aeromagnetic anomaly could be the signal of the buried huge iron ore bodies at depth in Panxi area, this has not been confirmed by deep drilling exploration. In order to solve this puzzle, we computed the aeromagnetic anomalies along profiles in the proven iron deposits of the Baima districts. The results reveal marked contrast between the calculated and observed anomalies. Based on these results and previous studies on the metallogenic features, we predict the presence of large iron ore bodies at depth beneath the Baima districts.

1 INTRODUCTION

The Panxi region has several large mafic-layered intrusions that host world-class Fe-Ti-V oxide deposits, such as the Panzhihua Fe-Ti-V deposit and Baima Fe-Ti-V deposit that form part of the ~260 Ma Emeishan Large Igneous Province. This region have attracted interest over the last decade because of their association with ore deposits(Zhou et al 2008) (Shellnutt et al., 2010) and the Panzhihua Fe-Ti-V oxide mine makes China a major producer of V and Ti, accounting for 6.7% and 35.2% of the total world production of V and Ti, respectively (Zhou et al., 2005).

Several models have been proposed for the formation of the Panzhihua deposit that are related to the Emeishan large igneous province (LIP): (1) the Panzhihua ore bodies developed concentrations of Fe and Ti through the fractional crystallization of ferrobaltic or ferropicritic magmas, followed by separation into silicate magma and Fe-rich oxide ore melt (Zhou et al., 2005); (2) early crystallization of

Fe-Ti oxides from a parent magma with 1.5 wt.% H₂O and oxide accumulated through crystal setting at the base of the intrusion (Pang et al., 2008; Zhou et al., 2008); and (3) an increase in magma fO₂ related to the CO₂-degassing of the footwall carbonates resulted in the accumulation of Fe-Ti oxides (Ganino et al., 2008). The Fe-Ti oxides had crystallized at an early stage of the solidification of the Panzhihua intrusion, in consideration of an effective accumulation of titanomagnetite in the Panzhihua intrusion (Ganino et al., 2008).

Although the depth of exploration conducted so far is shallow, there are some clues to indicate the presence of greatly potential iron ores at depth in the Panzhihua-Xichang area. He have suggested that the known deposits may not have appeared in their overlapping anomaly regions of 1:50,000 ΔT reduced-to-pole upwards vertical second derivative and ΔT reduced-to-pole downwards continuation ,the 3D model of Hongge Fe-Ti-V deposit was also built under the constrain of the drilling profiles and high- precision aeromagnetic data(Ganino and Arndt,

2009). Ge suggested that the deep levels beneath the Daheishan and Minzhengxiang districts are benefit space for future prospecting (Ge et al. 2015).

The interactive inversion technique on profile of magnetic anomalies is a new method that can be used to infer the depth and attitude of deeply buried ore bodies through geophysical data inversion, and has been successfully applied for the prediction of several iron ore bodies (Fan et al., 2010, 2012; Yu et al., 2007). To evaluate the possibility of deep iron ore bodies in these areas, we conducted 15 magnetic inversion lines across both Panzhihua area and Baima area, among them 10 magnetic inversion lines in Panzhihua area and 6 magnetic inversion lines in Baima area proved to be of obvious ore prospecting potential. The results from the inversion aid in evaluating the possibility of the presence of deep iron ore bodies and understanding the distribution of iron ore bodies in the Panzhihua-Baima area.

2 GEOLOGICAL SETTING

Numerous papers have described the geological setting of the ~260 Ma Emeishan Large Igneous Province and the large mafic-ultramafic intrusions that are considered to be part of the plumbing system of the Emeishan flood basalt (Zhou et al., 2008). The Emeishan magmas intruded sedimentary rocks of the Sichuan basin. In the Panxi region, uplift and erosion has exposed large mafic-ultramafic intrusions that are considered to be part of the plumbing system of the Emeishan flood basalts (Figure 1).

The Panzhihua gabbroic intrusion dips 50~60° NW and extends about 19 km along strike. The majority of the wall rocks are Neoproterozoic (Sinian) dolostones (Figure 2a). These rocks are almost pure and most contain very low contents of clay and silica minerals, but they are interbedded with siliceous limestones, marlstones and shales (Pêcher et al. 2013).

From stable isotope analyses, Ganino estimated that the Panzhihua gabbro assimilated 8~13.7 wt.% of carbonate wallrock (Ganino et al., 2013), and provided preliminary descriptions of the marbles and skarns and explained how carbon dioxide released during the metamorphism may have triggered both the ore formation and global climate change (Ganino et al., 2008). Magnetite-rich melanogabbro at the base grades through normal gabbro to leucogabbro near the top. The large Fe-Ti-V oxide ore deposits occur as magnetite-rich

cumulate layers or discordant lenses along the southeast margin of the intrusion. The contact aureole is >300 m thick and is mostly composed of brucite marble that formed from the thermal metamorphism of dolostones, and various calc-silicate rocks (olivine, diopside or garnet bearing marbles) that formed from marly layers. Banded carbonate-serpentinite reaction rims, “zebra-rocks”, surround small dolerite dykes that were probably the early intrusions associated with the emplacement of Panzhihua magma.

The Baima mafic layered intrusion is located in the central part of the Panxi area, SW China (Figure 1). The N-S striking intrusion is 24 km long and 2 km wide, dips to the west in 50–70°, and is emplaced into the Sinian metamorphic sandstone, phyllite, slate and marble (Figure 3). After emplacement, the Baima intrusion was surrounded and cut by ~259 Ma syenitic intrusions and dykes (Zhang, et al., 2012). In addition, several NW-SE-trending faults separate the Baima intrusion into five segments, including Xiajiaping, Jijiping, Tianjiacun, Qinggangping and Mablinglang (Figure 3). Along the strike, the Baima intrusion shows a thickness gradation from a more primitive facies in the north to a more evolved thinner facies in the south. The magnetite ore reserve of Baima intrusion is 1497 Mt (million ton) with mean grades of ~26% total Fe, ~7% TiO₂ and ~0.21% V₂O₅ (Zhang, et al., 2012).

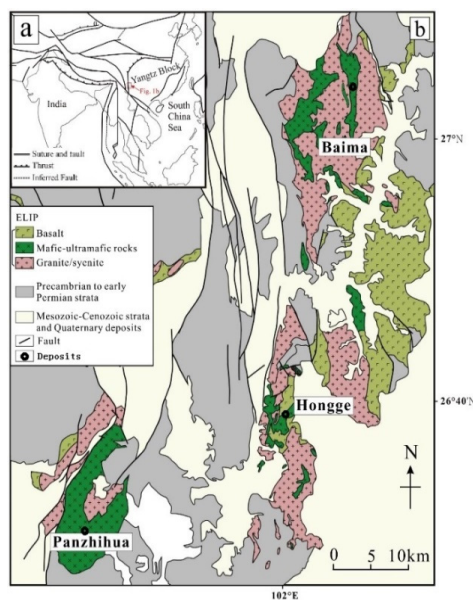


Figure 1: Simplified regional geology of the Panxi area, Emeishan large igneous province, SW China, showing the distribution of Panzhihua, Hongge and Baima mafic-ultramafic intrusions that host Fe-Ti-(V) oxide ore.

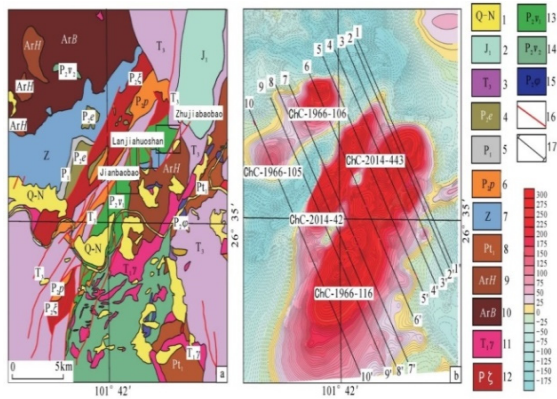


Figure 2: (a) Geological map of the Panzhihua area.; (b) aeromagnetic anomalies in the Panzhihua area; 1 – Quaternary~Neogene; 2 - Lower Jurassic; 3 - Upper Triassic; 4 - Middle Permian (Emeishan basalt); 5 - Lower Triassic; 6 - Middle Triassic phonolite; 7 - Sinian limestone and marble; 8 - Kangding complex Pianjiangtian unit; 9 - Kangding complex Huatan unit; 10 - Kangding complex Bude unit; 11 - Early Triassic granite; 12 – Permian Syenite; 13 - Middle Permian gabbro (containing seam); 14 - Middle Permian gabbro and dioritic; 15 - Middle Permian pyroxenite; 16 - Faults; 17 - Inversion profiles(5 low potential profiles in the northern part are not mentioned).

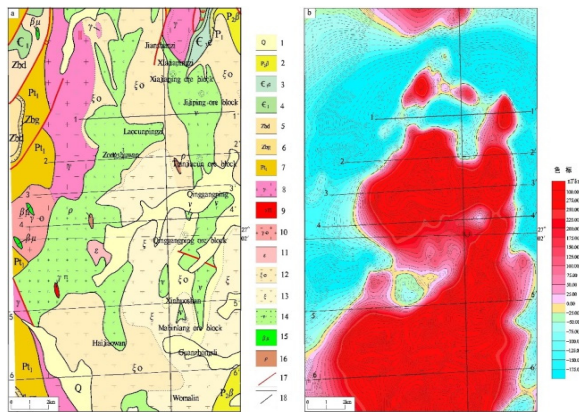


Figure 3. (a) Geological map of the Baima area.; (b) aeromagnetic anomalies in the Baima area; 1 – Quaternary; 2 - Middle Permian (Emeishan basalt); 3 - Upper Cambrian; 4 - Lower Cambrian; 5 - Sinian Dengying Formation; 6 - Sinian Guanyinya formation; 7 – Lower Proterozoic; 8 – Granite; 9 - Granite porphyry; 10 - Plagiogranite; 11 – Huangcao Syenite; 12 - Quartz syenite; 13 – Baima Syenite; 14 - Gabbro; 15- Dolerite; 16 - Diorite; 17- Faults; 18- Inversion profiles(9 low potential profiles in the southern part of this area are not mentioned).

3 GEOPHYSICAL SETTING

3.1 Characteristics of Magnetic Anomalies

On the 1:50,000 contour map of the aeromagnetic ΔT in Baima area (Figure 3b), several anomalies with an intensity 775~ 1200 nT is identified in the Baima area ,known iron ore belts is located along the S-N high magnetic anomaly zone. According to the contour map of the aeromagnetic ΔT , the area of the high magnetic anomalies is much larger than the iron ore belts. From Laocunpingzi to Womalin where iron deposits have not been found, the intensity of the aeromagnetic anomalies is more than 1000nT.

3.2 Physical Properties of Rocks and Ores

We measured the physical properties of selected iron ores, the ore bearing layers and cover strata, and the statistical results are listed in Table 1. The susceptibilities of the metamorphic rocks, sedimentary rocks and are in the range of $(0\sim 10) \times 10^{-5}$ SI, which can be generally regarded as non-magnetic. Gabbro (the ore bearing layer) shows a much higher susceptibility of $(11,768.79\sim 116.99) \times 10^{-5}$ SI. The susceptibilities of the iron ore are in the range of $(129,000\sim 20,499) \times 10^{-5}$ SI, which is a geological body that could cause a strong magnetic anomaly in this area, with densities in the range of $3.1\sim 4.2 \text{ g/cm}^3$.

Removing errors in measurement ,the relationship between Susceptibility and Ore grade is positive correlation (Sun et al,1991; Tian et al,2013).We conducted magnetic susceptibility measurement and optical film identification upon 30 magnetite samples (Figure 4) from Panzhihua deposit and Baima deposit , and the results indicated that the magnetic susceptibility can be used as the basis for the division of rich iron ores.

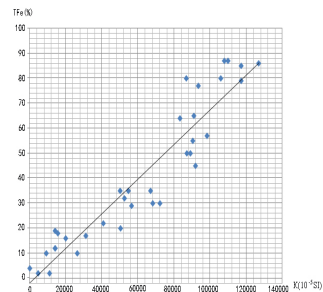


Figure 4. The relationship between susceptibility and ore grade in Panxi area.

Table 1: Physical properties of geological bodies.

| Name | Number of measured points | Susceptibility(10^{-5} SI) | | | area |
|---------------------|---------------------------|-------------------------------|---------------|---------------|----------------------------|
| | | Maximal value | Minimum value | Average value | |
| medium-grade ore | 32 | 116000 | 38090 | 76541 | Panzhuhua area |
| high-grade ore | 31 | 129000 | 55741 | 111521 | Panzhuhua area |
| Low-grade ore | 34 | 113000 | 20063 | 61041 | Panzhuhua area |
| Submarginal ore | 30 | 46062 | 20499 | 33618 | Panzhuhua area |
| Gabbro | 38 | 6539 | 2865 | 4564 | Panzhuhua area |
| Gabbro | 35 | 11768 | 116 | 6406 | Panzhuhua area(drill core) |
| Gabbro(ore bearing) | 30 | 19014 | 3483 | 11286 | Panzhuhua area |
| Gray marble | 33 | 10 | 0.2 | 0.7 | Panzhuhua area |
| Syenite | 32 | 3357 | 1508 | 2243 | Panzhuhua area |
| Phonolite | 32 | 4916 | 1815 | 3364 | Panzhuhua area |
| Basalt | 30 | 5556 | 807 | 4186 | Panzhuhua area |
| Sandstone | 31 | 12 | 0.4 | 5 | Panzhuhua area |
| granite gneiss | 30 | 1244 | 98 | 560 | Panzhuhua area |
| granite | 34 | 2011 | 104 | 1121 | Panzhuhua area |
| Pyroxenite | 30 | 15905 | 6428 | 11075 | Panzhuhua area |
| Low-grade ore | 31 | 89903 | 30004 | 59442 | Baima area |
| high-grade ore | 31 | 127000 | 20163 | 98134 | Baima area |
| Gabbro(ore bearing) | 32 | 26486 | 1063 | 9846 | Baima area |
| Gabbro | 36 | 10497 | 142 | 4983 | Baima area |
| Gray marble | 32 | 14 | 1.2 | 5.5 | Baima area |
| Syenite | 30 | 5669 | 2305 | 4323 | Baima area |
| Basalt | 30 | 5556 | 807 | 4057 | Baima area |
| Granite | 37 | 34 | 1 | 9 | Baima area |
| dolomite | 30 | 10.9 | 0.2 | 3.3 | Baima area |
| Sandstone | 31 | 11 | 1 | 3 | Baima area |
| granite gneiss | 32 | 53 | 2 | 14 | Baima area |

4 INTERACTIVE INVERSION TECHNIQUE OF MAGNETIC ANOMALIES ALONG THE UNDULATING TERRAIN PROFILE

Along undulating terrain profiles can be expressed in 2.5-D. The magnetic anomalies are calculated above the initial model with polygonal sections of level prism 2.5-D that are created on the basis of the known geological structures, the property data and semi-quantitative interpretation. Thereafter the model parameters continue to be adjusted until the calculated gravity and magnetic anomalies are

consistent with measured gravity and magnetic anomalies. Finally, based on these, we can understand some important information such as the depth, shape and volume of iron ore bodies (Fan et al., 2012).

Deep ore deposit prediction has been achieved by utilizing this technology (Cong et al., 2012; Fan et al., 2010, 2012; Yu et al., 2007). Yu noted that two iron ore bodies dipping to the south occur at 230–480 m and 630–880 m, with a horizontal distance of 200 m through the aeromagnetic anomaly inversion of Xiangbishan profile across Daye iron deposit in Hubei province, China. The borehole ZK21-8 exploration has successfully confirmed the inversion result (Fan et al., 2012),

several layered ore bodies with a total thickness of 14.6m at 40–45% Fe were found at a depth interval of 740–840 m, consistent with the above prediction.

4.1 Calculation Method for Magnetic Anomalies

The three-components of magnetic field for any point P (x, y, z) on the section of the level prism 2.5-D could be calculated by the formula (Fan et al., 2010):

$$H_{ax}(P) = -\sum_{i=1}^N \sin \varphi_i (J_x I_{1i} + J_y I_{2i} + J_z I_{3i}) \quad (1)$$

$$H_{ay}(P) = -\sum_{i=1}^N (J_x \sin \varphi_i - J_z \cos \varphi_i) I_{2i} - J_y ((\sin \varphi_i I_{1i} - \cos \varphi_i I_{3i})) \quad (2)$$

$$Z_a(P) = -\sum_{i=1}^N \cos \varphi_i (J_x I_{1i} + J_y I_{2i} + J_z I_{3i}) \quad (3)$$

which can be further calculated as:

$$I_{ji} = P_{ji}(Y_2) - P_{ji}(Y_1), j = 1, 3 \quad (4)$$

$$P_{1i}(y) = \cos \varphi_i \ln \frac{R_i+y}{R_{i+1}+y} - \sin \varphi_i \left(\arctan \frac{U_{i+1}y}{w_i R_{i+1}} - \arctan \frac{u_i y}{w_i R_i} \right) \quad (5)$$

$$P_{2i}(y) = \ln \frac{u_i+R_i}{u_{i+1}+R_{i+1}} \quad (6)$$

$$P_{3i}(y) = \cos \varphi_i \ln \frac{R_i+y}{R_{i+1}+y} - \cos \varphi_i \left(\arctan \frac{U_{i+1}y}{w_i R_{i+1}} - \arctan \frac{u_i y}{w_i R_i} \right) \quad (7)$$

The magnetic anomaly of the total field is:

$$\Delta T(P) = H_{ax}(P) \cos I_0 \cos D_0 + H_{ay}(P) \cos I_0 \sin D_0 + Z_a(P) \sin I_0 \quad (8)$$

which can be further calculated as:

$$u_i = x_i \cos \varphi_i + Z_i \sin \varphi_i, u_{i+1} = x_{i+1} \cos \varphi_i + Z_{i+1} \sin \varphi_i \quad (9)$$

$$R_i = (x_i^2 + y^2 + z_i^2)^{1/2}, R_{i+1} = (x_{i+1}^2 + y^2 + z_{i+1}^2)^{1/2} \quad (10)$$

$$\varphi_i = \arctan \frac{z_{i+1}-z_i}{x_{i+1}-x_i}, w_i = -x_i \sin \varphi_i +$$

$$z_{i+1} \cos \varphi_i \quad (11)$$

$$J_x = J \cos I \cos D, J_y = J \cos I \sin D, J_z = J \sin I_0$$

where, I_0 : geomagnetic inclination and D_0 : geomagnetic declination; i : prism corner number; N : prism side number; J : prism magnetization; I : prism magnetic inclination and D : prism magnetic declination. Because the formula applies to arbitrary points on the section, we infer

that it may be applied to almost all undulated terrains.

4.2 The Interactive Inversion Software

The interactive inversion software used in this study is called GMVPS (Sui et al., 2004). It simulates the underground geological conditions at deep level by creating a model or multiple models that consist of finite horizontal prisms with a section of arbitrary polygons. The corner number of the polygons may be added, reduced or moved based on the known geological structures and anomaly characteristics. In addition to inductive susceptibility, inductive magnetic inclination, inductive magnetic declination, residual magnetization, residual inclination, horizontal extension of the model and pattern of the polygonal section, some other relevant parameters, including geomagnetic field strength, geomagnetic inclination, geomagnetic declination, profile azimuth, are also entered and corrected in the dialog box. The computational curve above the model is updated in real time as the change of the model parameters (Fan et al., 2010). The shape of the model is terminated at the least difference between the calculated and measured anomalies. Thus, we can get the final model by an inversion result (Figure 5 as an example). The physical properties used in the software is given according to the physical properties measured (table 2).

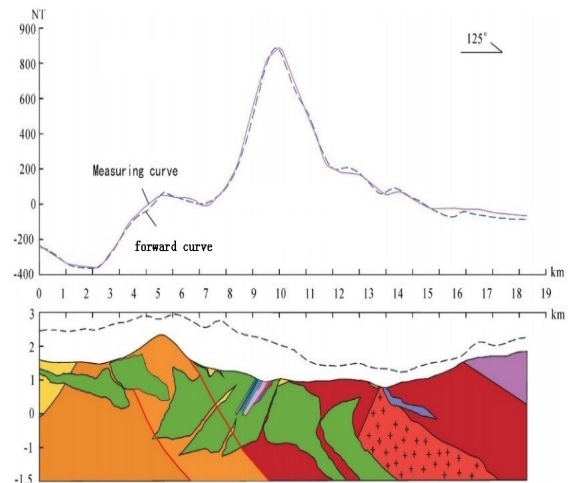


Figure 5: Aeromagnetic anomaly caused by the proven Panzihua iron deposit along Panzihua 4-4 'profile (Figure legend refer to figure 7).

Table 2: Physical properties used in software.

| Area | Name | Susceptibility $\kappa(10^{-5}SI)$ | Effective magnetization $J_s(10^{-3}A/m)$ | direction of magnetization; $(^\circ)$ | Density $(10^3g/cm^3)$ |
|----------------|---|---------------------------------------|--|--|---------------------------|
| Baima area | Gabbro(ore bearing) | 9840 | 3761.79 | 41.7 | |
| | Gabbro | 4983 | 1927.45 | 41.7 | |
| | Gray marble and dolomite | 5.5 | 2.2 | 41.7 | |
| | Syenite(mixed with gabbro) | 4320 | 1698.26 | 41.7 | |
| | Syenite | 1850 | 727 | 41.7 | |
| | Basalt | 4050 | 1552.81 | 41.7 | |
| | Sandstone and siltstone | 3 | 1.2 | 41.7 | |
| | Archean and Proterozoic metamorphic rocks | 14 | 5.6 | 41.7 | |
| | Granite | 9 | 3.6 | 41.7 | |
| | High grade ore (more than 45%) | 98100 | 37778.5 | 47 | 4.0 |
| | Low grade ore (<45%) | 59442 | 23367.6 | 47 | 3.2 |
| Panzhuhua area | Gabbro(ore bearing) | 11200 | 4288.99 | 40.9 | |
| | Gabbro | 5600 | 2144.5 | 40.9 | |
| | Pyroxenite | 11075 | 4270 | 40.9 | |
| | Gray marble and dolomite | 0.7 | 0.3 | 40.9 | |
| | Syenite | 2243 | 857.79 | 40.9 | |
| | Phonolite | 3364 | 1286.7 | 40.9 | |
| | Basalt | 4486 | 1715.6 | 40.9 | |
| | Sandstone and siltstone | 5 | 2 | 40.9 | |
| | Archean and Proterozoic metamorphic rocks | 560 | 214.449 | 40.9 | |
| | Granite | 1121 | 428.99 | 40.9 | |
| | grade I ore (TFe \geq 45%) | 111060 | 42890 | 53.0 | 4.2 |
| | grade II ore (44.9% \geq TFe \geq 30%) | 76500 | 30022 | 53.0 | 3.7 |
| | grade III ore(29.9% \geq TFe \geq 20%) | 61000 | 23503.6 | 53.0 | 3.4 |
| | Submarginal ore(19.99% \geq TFe \geq 15%) | 33600 | 12867 | 53.0 | 3.1 |

5 RESULTS

The parameters of the normal maetic field of the Panxi area used in the interactive inversion are the following: geomagnetic field strength = 48,202 nT,

geomagnetic inclination = 40.9°, geomagnetic declination = -1.4°, and profile azimuth= 125°(Panzhuhua)/90°(Baima). The initial model is built on the basis of cross sections (Figure 6 and Figure 7 for example).

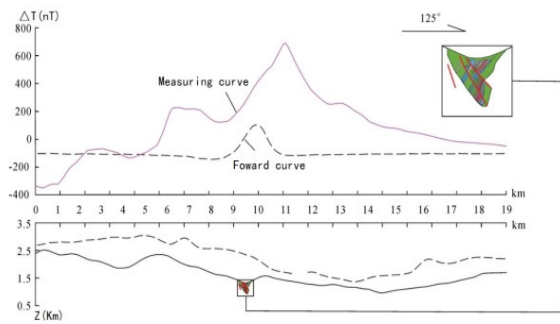


Figure 6: Aeromagnetic anomaly caused by the proven Panzhihua iron deposit along Panzhihua 4-4 'profile (Figure legend refer to figure 8).

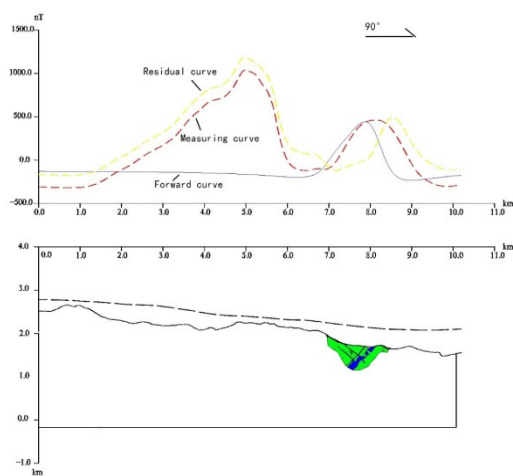


Figure 7: Aeromagnetic anomaly caused by the proven Baima iron deposit along Baima 2-2 'profile (Figure legend refer to figure 9)

5.1 Aeromagnetic Anomaly Caused by the Proven Panzhihua Iron Deposit

The salient features of the Panzhihua iron deposit (Figure 6 and Figure 8) are summarized as follows. The exploration depth is ~600 m. The ore body is ~200m thick, ~5000m long, and dips to the northwest at dipping angle of 50°. The wall rocks around the ore body are mainly Permian gabbro which intruded into Simian limestone and Archean gneiss.(Figure 6 and Figure 8).

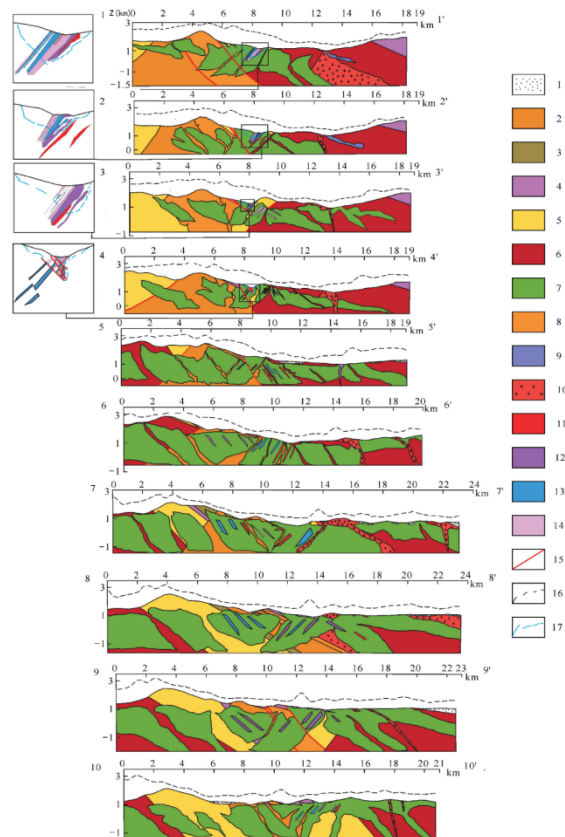


Figure 8: Inversion profiles 1~10 in Panzhihua area.

1- Quaternary; 2 - Permian phonolite; 3 - Permian basalt; 4 - Triassic sandstone; 5 - Sinian limestone; 6 - Archean, Proterozoic metamorphic rocks; 7 - Gabbro; 8 - Syenite; 9 -Pyroxenite; 10 - Granite; 11 - Grade I ore (TFe≥45%); 12 - Grade II ore (TFe 30~44.9%); 13 - Grade III ore (TFe20~29.9%); 14 - Submarginal ore (TFe15~19.9%); 15 - faults; 16 - Flight trajectory; 17 - Drilling controlled part.

On the basis of physical properties and aeromagnetic anomaly features, the aeromagnetic anomaly can be accomplished by running GMVPS, and is shown on the geological section of the proven Panzhihua iron deposit (Figure 6 and Figure 8). The physical properties of the rock and the ore data for modeling are listed in Table1 and shown in Figure 7.

5.2 Aeromagnetic Anomaly Caused by the Proven Baima Iron Deposit

The salient features of Baima iron deposit (Figure 7 and Figure 9) are summarized below. The exploration depth is ~430 m. The ore body is ~200 m thick, ~13000 m long(cut and translated by faults

into more than 5 ore blocks), and dips to the west at a dipping angle of 70°. The wall rocks around the ore body are mainly Permian gabbro(Figure 7 and Figure 9). We calculate the aeromagnetic anomaly of the Baima iron deposit via the abovementioned method (Figure 7 and Figure 9).The physical parameters of the rocks and ores for modeling are listed in Table 1 and shown in Figure 9.

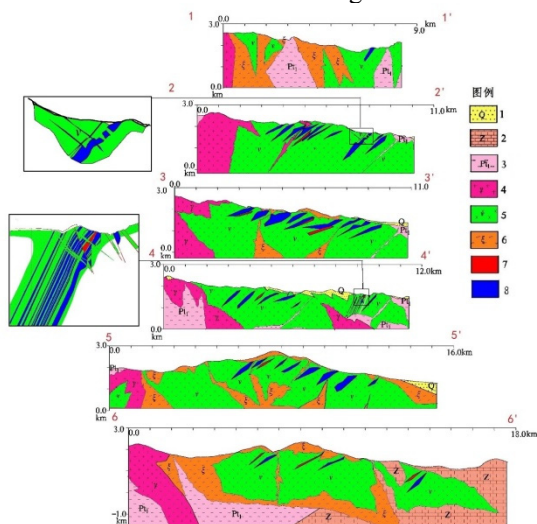


Figure 9: Inversion profiles 1~6 in Baima area(Cross sections were showed in the enlarged views)

1- Quaternary; 2 - Sinian limestone; 3 - Proterozoic; 4 - Granite; 5 - Gabbro; 6 – Syenite;7 - Rich ore(TFE≥45%); 8 - Lean ore(TFE<45%).

5.3 Results of Interactive Inversion on Magnetic Anomalies along Panzhihua and Baima Profiles

Based on the range of physical properties for rocks and ores in the Panzhihua and Baima area, we can get these physical parameters for modeling (Table 1). The parameters listed in Table 2 indicate magnetite ores are the strongest magnetic, and the ore-bearing layers(mainly gabbro) display the transition between non-magnetic or weakly magnetic limestone and syenite. However, the strength and the center position of magnetic anomalies significantly depend on the shapes of iron bodies. To obtain the best results, we corrected the models of the iron ore bodies constantly, until the residual anomaly between aeromagnetic fitting curve and the measured curve is the minimum. Consequently, when the aeromagnetic residual anomalies are the least, we can obtain the final model for Panzhihua and Baima profiles (Figure 8 and Figure 9).

6 DISCUSSION

6.1 Deep Mineral Exploration in the Panzhihua and Baima Area

Several magmatic Fe-Ti-V oxide deposits in the Panxi region, SW China, are hosted in layered mafic-ultramafic intrusions of the Emeishan Large Igneous Province(ELIP) (Figure 1) (Zhong et al., 2002; Zhou et al., 2005). Examples are the giant deposits of Panzhihua, Hongge and Baima. The Hongge deposit alone contains 4572 Mt of ore reserves with 1830 Mt of Fe, 196 Mt of Ti and 14.7 Mt of V (Ganino et al., 2013). In addition to these three giant deposits, other deposits currently being mined include the Taihe deposit to the north of the Baima deposit. In recent years, With the continuous development of the prospecting work ,several deposits, including Anyi , Mianhuadi and Wuben, were discovered.

Our investigation suggests that there are potential targets for iron ore exploration in the Baima area. As shown in Figure 6 and 7, the calculated aeromagnetic anomalies are much lower than the observed anomalies in Baima deposit. The similar scenario can also be seen in the other inversion lines in Panzhihua and Baima area (Figure 8 and Figure 9,curves were omitted). It suggests that there might be buried large-scale iron ore bodies both in Panzhihua and Baima, because such large measured anomalies cannot be produced by the proven iron ore bodies or the gabbro surrounded them. The Panzhihua and Baima iron ore bodies extend to larger depth level and as shown in Figure 7 and 8. On the whole, the Panzhihua and Baima iron deposit consists of a several layered iron bodies.

The proven iron ore bodies of Panzhihua iron deposit are situated on the southeast part of the iron ore layers and the volume only accounts for ~50% of the volume predicted by the inversion result. Therefore, we believe that there is a great potential to discover large iron ore bodies beneath the Panzhihua and Baima area. The exact results of the prospecting targets of Panzhihua and Baima area were confirmed according to the top projection of the inferred iron ore layers and the vertical first derivative of the magnetic field(Figure 10). According to the study, profiles 1-1', 2-2', 3-3' , 4-4'and 5-5' in Panzhihua have little potential in finding new iron ore deposits near-surface, only deep ores delow the known deposits are expectable.Profiles 6-6', 7-7', 8-8' and 9-9' proved to be most potential for the iron ore in Panzhihua area for the large volume according the study.

Similarly, profiles 2-2', 3-3', 4-4', 5-5' and 6-6' proved to be most potential for the iron ore in Baima area.

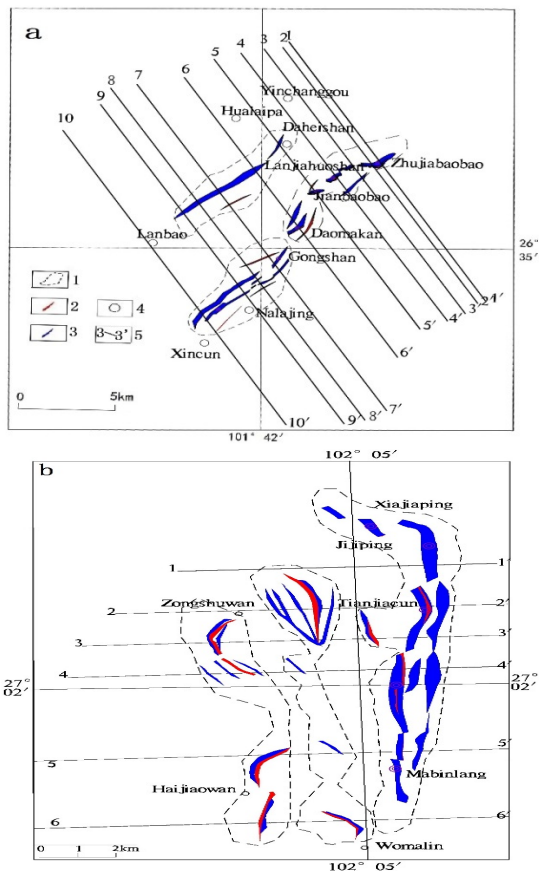


Figure 10: Prospecting targets in Panzhihua and Baima area. 1- Prospecting area; 2 - Prospecting targets(Rich ore); 3 - Prospecting targets(Lean ore); 4 - Locations; 5 - Inversion profiles.

6.2 Shape of Rock Bodies and Its Relationship with Ore Grade in the Panzhihua and Baima Area

Comparing the similarity and diversity between Panzhihua and Baima iron deposit, we concluded that the controlling factors of mineralization are similar: (1)the crystallization of Fe-Ti oxides from iron rich mafic magma in the earlier stage is the prerequisite of mineralization; (2)Gravity separation is the physical mechanism of the formation of Fe Ti oxide ore of vanadium titanium magnetite.

After the parent magma separated into silicate magma and Fe-Ti rich oxide ore melt (Zhou et al., 2005), the Fe-Ti rich magma migrated into Panzhihua and Baima rock body, Olivine, plagioclase and Fe-Ti oxides become liquidus

minerals, forming magnetite ore layer under the gravity variation.

According to the inversion results(Figure 8 and Figure 9),the shapes of Panzhihua rock body and Baima rock body show different characteristics in geometrical forms .In Panzhihua area , as a result of the obvious concave section at the bottom of the magma chamber and the smaller horizontal area of single rock body, the gravity separation of magnetite is more abundant in the process of magmatic flow, leading to the formation of thick massive ore(richer ore) in Zhujiaobaobao area. Relatively speaking,in Baima area the bottom of the magma chamber is relatively gentle, and the horizontal area of single rock body is larger , gravity separation is not abundant ,thus formed dense disseminated ore(leaner ore).

6.3 Genesis of Panzhihua Type V-Ti Magnetite Deposits

Different explanations were given for the ore forming processes including immiscibility (Zhou et al., 2005), fractionation (Pang et al., 2008) and assimilation (Ganino et al.,2008). Large contact aureoles, mostly composed of brucite marbles and calc-silicate rocks, developed at the contact of the intrusions (Zhou et al., 2008).

Based on the inversions we conducted, we measured the length of the contact aureole on each inversion profiles to make some conservative estimates of the dimensions of the part of the aureole that underwent partial decarbonatization, the thickness was estimated as 300 m. The volume of the aureole between two profiles can be calculated as prismoid or frustum of a pyramid, giving a total volume of 13.6 km³. If the rock density is 2,750 kg/m³, the mass of the dolomite was 37.5Gt. If we assume that 80% of dolomite is transformed into brucite, then 190 g of CO² is released for each kilogram of rock (Ganino et al., 2008).The total amount of CO² is calculated as 5.7 Gt, which is similar to result Ganino obtained. However,90% of the aureole on the inversion profiles were located near Hualaipia area, 6.2 kilometers northwest of the panzhihua deposit. Although large volume of blinded gabbro were inferred in Hualaipia area, based on the inversions, the metallogenic potential is low. How CO²-rich fluids Interacted with the magma is hard to estimate, and the inversions above does not support the view that assimilation with carbonate rocks is vital condition in the formation of Panzhihua type V-Ti magnetite deposits.

7 CONCLUSIONS

Computation through forward and inverse methods of the magnetic anomalies of Panzhihua and Baima profiles have been conducted through interactive inversion technique. Our study leads to the following three major conclusions.

There is a potential to find large-sized iron ore bodies buried at depth in the Panzhihua and Baima area that remain to be discovered, the inversions we conducted provides prospecting targets for mineral exploration. According to the study, profiles 6-6', 7-7', 8-8' and 9-9' in Panzhihua area and Profiles 2-2', 3-3', 4-4', 5-5' and 6-6' in Baima area proved to be most potential for the iron ore.

The Panzhihua iron deposit is composed of thick massive ore and disseminated ore, while in Baima deposit only disseminated ore was found. The inversions indicated that such phenomenon could be explained by the different shapes of different magma chamber which related to the process of gravity separation of magnetite.

Based on the inversions, the quality of CO₂ released from dolomite that underwent partial decarbonatization is ~37.5Gt. Most of the aureole is located beneath Hualaipa area where the metallogenic potential is low, which probably mean that assimilation with carbonate rocks is not the vital condition in the formation of Panzhihua type V-Ti magnetite deposits.

ACKNOWLEDGEMENTS

Financial support for this work was provided by the The national key research projects(2017YFC0602206), 973 Program(Grant No. 2012CB416805) and Projects of the China Geological Survey Bureau Program (DD20160066,DD2016006637).

REFERENCES

Fan Z G , Xu Z H, Tan L, Yang X, Zhang H R, Zhou D Q, Liu Q K and Tan L 2014 A study of iron deposits in the Anshan area, China based on interactive inversion technique of gravity and magnetic anomalies *Ore Geology Reviews* **57** 0618–0627

- Ganino C and Arndt N T 2009 Climate changes caused by degassing of sediments during the emplacement of large igneous provinces *Geology* **37** 323-326
- Ganino C, Arndt N T, Zhou M F, Gaillard F and Chauvel C 2008 Interaction of magma with sedimentary wall rock and magnetite ore genesis in the Panzhihua mafic intrusion, SW China *Mineralium Deposita* **43** 677-694
- Ganino C, Harris C, Arndt N T, Prevec S A and Howarth G H 2013 Assimilation of carbonate country rock by the parent magma of the Panzhihua Fe-Ti-V deposit (SW China): evidence from stable isotopes *Geoscience Frontiers* **4** 547-554
- Ge T F, Fan Z G, Huang X Z, Zhang Y J, He J Z and Li J J 2015 Deep metallogenic potential and prospecting direction of Panzhihua V-Ti-magnetite deposit determined from aeromagnetic data analysis *Geology an Exploration* **51(6)** 1041-1048 (in Chinese with English abstract).
- He J Z, Fan Z G, Huang X Z, Ge T F and Yang R 2015 Three-dimensional inversion of magnetic data and geological modeling for the Hongge iron deposit *Geology and Exploration* **51(6)** 1049-1058 (in Chinese with English abstract)
- Pang K N, Li C, Zhou M F and Ripley E M 2008a. Abundant Fe-Ti oxide inclusions in olivine from the Panzhihua and Hongge layered intrusions, SWChina: evidence for early saturation of Fe-Ti oxides in ferrobaltic magma *Contributions to Mineralogy and Petrology* **156** 307-321
- Pêcher A, Arndt N T, Bauville A, Zhou M F and Ganino 2013 Structure of the Panzhihua Fe-Ti-V Deposit, China *Geoscience Frontiers* **4** 571-581
- Shellnutt J G, Wang K L, Zellmer G F, Iizuka Y, Jahn B-M, Pang K-N, Qi L and Zhou M-F 2011 Three Fe-Ti oxide ore-bearing gabbro-granitoid complexes in the Panxi region of the Emeishan large igneous province, SW China. *American Journal of Science* **311** 773-812
- Sui S W, Yu C C and Yao C L 2004 The semi-intelligent processing and interpretation software for gravity and magnetic anomalies along the profile of rolling topography and its application *Geophys. Geochem. Explor.* **28 (1)** 65–68 (in Chinese with English abstract).
- Sun D M 1991 Application of magnetic susceptibility meter in quality inspection of magnetite. *Metal Mine* **1** 9-11(in Chinese)
- Tian J and Fan M Q 2013 The mathematical model of correlation between magnetic material content and TFe grade in magnetite *China Mining Magazine* **22(10)** 105-108(in Chinese)

- Yu C C, Fan Z G, Wang N D, Xiong S Q, Wan J H and Zhang H R 2007 High-resolution aeromagnetic exploration methods and their application in Daye iron mines *Prog. Geophys.* **22** (03) 979–983 (in Chinese with English abstract)
- Zhang X Q, Song X Y, Chen L M and Xie W 2012 Fractional crystallization and the formation of thick Fe–Ti–V oxide layers in the Baima layered intrusion, SW China *Ore Geology Reviews* **49** 96–108
- Zhou M F, Arndt N T, Malpas J, Wang C Y and Kennedy A K 2008 Two magma series and associated ore deposit types in the Permian Emeishan large igneous province, SW China *Lithos* **103** 352–368
- Zhou M F, Arndt N T, Malpas J, Wang C Y and Kennedy A K 2008 Two magma series and associated ore deposit types in the Permian Emeishan large igneous province, SW China. *Lithos* **103** 352–368
- Zhou M F, Robinson P T, Leshner C M, Keays R R, Zhang C J and Malpas J 2005 Geochemistry, petrogenesis and metallogenesis of the Panzhihua gabbroic layered intrusion and associated Fe-Ti-V deposits, Sichuan Province, SW China *Journal of Petrology* **46** 2253–2280